

# Error reduction methods for local maximum filtering of high spatial resolution imagery for locating trees

Mike Wulder, K. Olaf Niemann, and David G. Goodenough

**Abstract.** Tree crown recognition using high spatial resolution remotely sensed imagery provides useful information relating the number and distribution of trees in a landscape. A common technique used to identify tree locations uses a local maximum (LM) filter with a static-sized moving window. LM techniques operate on the assumption that high local radiance values represent the centroid of a tree crown. Although success has been found using LM techniques, various authors have noted the introduction of error through the inclusion of falsely identified trees. Missing trees, or omission error, are primarily the result of too coarse an image spatial resolution in relation to the size of the trees present. Falsely indicated trees (commission error) may be removed through image processing post-LM filtering. In this paper, using 1-m spatial resolution multi-detector electro-optical imaging sensor (MEIS-II) imagery of a study location on Vancouver Island, British Columbia, we present a variety of techniques for addressing commission error when applying an LM technique. Methods exploiting spatial and spectral information are applied. As a benchmark, LM generated within a  $3 \times 3$  window with no commission error reduction resulted in a 67% overall accuracy, with a 22% commission error. The results of the commission error reduction must be considered against resultant overall accuracy. Using variable window sizes, as suggested by image spatial structure, for the generation of LM provided for the maintenance of similar overall accuracy (62%) with a decrease in commission error (to 11%).

**Résumé.** La reconnaissance de la couronne des arbres à l'aide d'images de télédétection à haute résolution spatiale apporte une information utile quant au nombre et à la distribution des arbres dans le paysage. Une des techniques utilisées couramment pour déterminer la localisation des arbres utilise un filtre de maximum local (ML) avec une fenêtre mobile à dimension statique. Les techniques de ML opèrent sur la prémisse que les valeurs élevées de radiance locale représentent le centroïde de la couronne d'un arbre. Quoique les techniques de ML aient connu du succès, divers auteurs ont observé que cette procédure introduit des erreurs qui se manifestent par l'inclusion d'arbres identifiés faussement. Les arbres manquants, ou erreur d'omission, sont principalement le résultat d'une résolution spatiale trop grossière par rapport à la dimension des arbres en présence. Les arbres identifiés faussement (erreur de commission) peuvent être éliminés au moyen d'un traitement d'image basé sur le filtrage post-ML. Dans ce texte, basé sur l'utilisation d'images MEIS-II à une résolution spatiale de 1 m d'un site d'étude situé sur l'île de Vancouver, en Colombie britannique, nous présentons diverses techniques visant la réduction de l'erreur de commission par le biais de l'application de la technique de ML. On applique des méthodes qui exploitent l'information spatiale et spectrale. À titre de référence, des ML générés à l'intérieur d'une fenêtre de  $3 \times 3$  sans réduction d'erreur de commission ont permis d'atteindre une précision globale de 67%, avec une erreur de commission de 22%. Les résultats de la réduction de l'erreur de commission doivent être considérés par rapport à la précision globale résultante. L'utilisation de fenêtres de dimension variable, en fonction de la structure spatiale de l'image, pour générer des ML a permis de conserver une précision globale semblable (62%) avec une réduction d'erreur de commission (jusqu'à 11%).

[Traduit par la Rédaction]

## Introduction

Aerial photography is still the most commonly used method of providing remotely sensed data for the characterization of forests. Yet, due to increasing information requirements, a decrease in the usefulness of aerial photographs for forest inventory purposes has been cited (Hyypä et al., 2000). The commercial availability of high spatial resolution satellite data (Tahu et al., 1998) has further spurred the development of digital techniques for the extraction of forest information. The full potential of high spatial resolution imagery in forestry will only likely be approached through automation of the image processing (Gougeon, 1995a). The information content of high spatial resolution imagery, where there are many pixels per

object, has resulted in the development of a range of techniques, such as valley following (Gougeon, 1995b), threshold-based spatial clustering (Culvenor, 2002), template matching (Pollock, 1996; Larsen and Rudemo, 1997; Larsen,

---

Received 3 January 2001. Accepted 8 May 2002.

**M. Wulder<sup>1</sup> and D.G. Goodenough.** Pacific Forestry Centre, Canadian Forest Service, Natural Resources Canada, 506 West Burnside Road, Victoria, BC V8Z 1M5, Canada.

**K.O. Niemann.** Department of Geography, University of Victoria, Victoria, BC V8W 3P5, Canada.

<sup>1</sup>Corresponding author (e-mail: mike.wulder@pfc.cfs.nrcan.gc.ca).

1999), mathematical morphology (Walsworth and King, 1999), and local maximum filtering (Pinz, 1999).

View angle, illumination angle, tree geometry, and bidirectional reflectance combine to result in a variation of the intensity of pixel digital numbers (DN) at different locations within an individual tree crown (Leckie et al., 1992). The radiance values also vary as a function of the tree crown depth, where the intensity is greatest near the tree centre and lessens towards the crown edges (Li and Strahler, 1992). As a result, individual trees may be discerned as localized regions of high DN values (**Figure 1**). In the case of coniferous trees, the contrast in DN values results in a local maximum (LM) value found at, or near, the centre of trees. In LM filtering, a window is passed over all pixels in an image to determine if a given pixel is of higher reflectance than all other pixels within the window (Dralle and Rudemo, 1997). Pixels identified with the highest DN value within the window are designated as tree locations. When a window of a fixed size is passed over an image it does not account for the presence of trees with different crown sizes, i.e., static-sized windows do not take into account the object-resolution relationship that exists between the trees (objects) and the image spatial resolution.

Observation of changing omission and commission errors as a function of crown radii provides an indication of the relationship between tree size and image resolution required to resolve individual trees with an LM filter. The distribution of error by tree size is important, as the large trees account for a greater proportion of the stand basal area than the smaller trees. An investigation of the success of tree identification by tree crown radius demonstrates the relationship between image

spatial resolution and LM filtering success. At an image spatial resolution of 1 m, a tree crown radius of 1.5 m appears to be the minimum size for reliable identification of tree locations using LM filtering (Wulder et al., 2000).

At the 1-m spatial resolution, there are too few pixels within the smallest,  $3 \times 3$  pixel, filter size to locate smaller trees. Yet, if the larger trees in the stand are consistently located, it may be possible to account for most of the stand basal area. Wulder et al. (2000) demonstrated that commission error resulted in the overestimation of basal area. In some cases, reducing commission error may come at the cost of increasing omission error. The increase in omission error is rationalized, as the trees that are "lost" with decreased commission are usually small, accounting for a small amount of the total stand basal area. The trade-off between total proportion of trees correct and the level of commission error allows the user to determine which is more important based on the intended use of the LM filter generated tree locations. The presentation of a process to estimate basal area from the LM filter generated tree locations demonstrated that slightly lower proportions of successful stem identification may be quite acceptable, as the majority of basal area is accounted for by large trees (Wulder et al., 2000), and achieving a minimum of commission error is more important.

Omission error with the LM technique is largely a function of image spatial resolution. Additional detection errors may arise from factors such as close proximity of neighbors, trees being located under other trees, shadows, or trees having low spectral contrast with respect to the understorey vegetation. As a result, a primary aim when applying LM filters is to maximize the number of legitimate trees found while also minimizing those falsely identified.

The hypothesis of the research is that commission error can be reduced through a variety of image-processing techniques exploiting both image spectral and image spatial information. The reduction of commission error may come at the expense of overall accuracy. The user must decide, based on their application, what is more important to avoid, the inclusion of non-existent trees, or missing actual trees. This paper focuses on minimizing the commission error, or false positives, identified using an LM filter, while attempting to maintain overall accuracy levels. To reduce commission error we apply and present the consequences of (i) variable window sizes, (ii) a spectral threshold and local variance within an LM window, (iii) a spatial-dependence threshold, and (iv) LM filtering of spatial-dependence data. The results of processing with the error reduction methods are compared to benchmark fixed-window LM processing with no error reduction applied.

## Methods

### Study area

The Greater Victoria Watershed is located at  $48^{\circ}23'N$  latitude and  $123^{\circ}41'W$  longitude, which is northwest of Victoria, British Columbia. Within this watershed, a 0.72-ha study area was selected with little topographic variability, composed of a

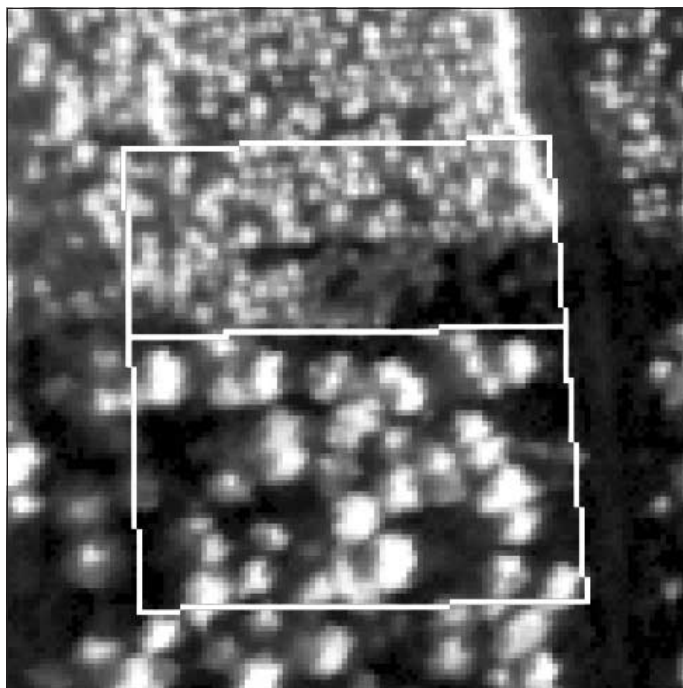


**Figure 1.** MEIS-II simulated panchromatic imagery, including notation of plantation (top rectangle) and mature (bottom rectangle) stands in the study area.

40-year-old plantation and a 150-year-old naturally regenerating mature stand (Hugh Hamilton, Ltd., 1991). The plantation (planted in 1965 and thinned in 1975) is composed of trees ranging in height from 8.6 to 25 m and is a mixture of Douglas-fir (*Pseudotsuga menziesii*) and western red cedar (*Thuja plicata*). The mature stand contains trees from 140 to 250 years of age ranging in height from 20 to 70 m and is dominated by Douglas-fir. Also present in the study site is a dense layer of understorey consisting of hemlock (*Tsuga heterophylla*), some red alder (*Alnus rubra*), salal (*Gaultheria shallon*), sword fern (*Polystichum munitum*), Oregon grape (*Mahonia nervosa*), and Oregon beaked moss (*Kindbergia oregana*).

### Field data

The 0.72-ha study area was partitioned into 72 grid cells of 10 by 10 m within which all trees were measured and located to 0.1 m of precision to allow for the creation of a stem map. In total, 209 trees were located, with 159 trees in the plantation stand and 50 trees in the mature stand. As part of the fieldwork for Hay and Niemann (1994), crown radius, diameter at breast height (DBH), species type, tree height at crown apex, and height at maximum crown radius were measured.

### Image data

The second-generation multi-detector electro-optical imaging sensor (MEIS-II) (Till et al., 1983) was flown at an altitude of 1428 m over the study site at 11:30 hours PST on 2 September 1993, with a resulting ground pixel size of 1 m (all images resampled to 720 pixels across track). The raw data were geometrically corrected using British Columbia Ministry of Environment Terrain Resource Information Management (TRIM) digital elevation data with a horizontal accuracy of  $\pm 20$  m. Solar altitude and azimuth angles at the time of the flight were 52° and 133°, respectively.

The MEIS-II is a pushbroom scanner with a temperature-stabilized, charge-coupled device (CCD) linear array and a spectral range from 380 to 1100 nm. Within the 720-nm spectral range, six user-defined, nadir-looking channels may be selected by mounting filters in front of the lens. A panchromatic channel was simulated by averaging the six available channels to summarize the spectral response found over the MEIS-II range from 432.85 to 847.65 nm (**Figure 1**). This enables a comparison with the 1-m panchromatic image data available on the IKONOS satellite (Mangold, 1999) (with a 450–900 nm panchromatic channel). Additionally, in previous work it was evident that there was no statistically significant difference between the results the LM generated from differing spectral channels (Wulder et al., 2000).

### LM filtering procedure

Individual trees can be discerned, in medium to dense forested areas, in high spatial resolution imagery as regions of high reflectance. The spatial structure of this reflectance, for

conifers, results in an LM value found at, or near, the centre of trees. In LM filtering, a window is passed over all pixels in an image to determine if a given pixel is of higher reflectance than all other pixels within the window (Dralle and Rudemo, 1997). Pixels identified as the largest DN value within the window are noted as tree locations.

### Variable window sizes

#### Semivariance

Semivariance is a well-understood and frequently applied image-processing technique in remote sensing (Curran and Atkinson, 1998). Semivariograms provide a means of measuring the spatial dependency of continuously varying phenomena. Variable window sizes are suggested for each pixel location based on an average semivariance range value computed from transects in the eight cardinal directions around each pixel in the image (Franklin et al., 1996). If there is spatial structure in a given data set, a semivariogram will reveal that semivariance rises until reaching the sill, which indicates the maximum variability between pixels. The range is the number of lags, or distance, to the sill (Curran and Atkinson, 1998). Therefore, within the range spatial dependence between pixel values is indicated. To minimize the potential effects of image anisotropy, image semivariance is computed for all eight cardinal directions from the central pixel, with the average of the eight results stored in a new image channel. Computing an average range value for each pixel in the image reduces problems that arise when attempting to select a representative single transect origin and angle (Wulder et al., 1998).

The conversion of semivariance ranges to window sizes requires user intervention (Wulder et al., 2000). The inter-pixel variability is limited at a 1-m spatial resolution, particularly in dense homogenous stands, which results in ranges that characterize the stand spatial dependency rather than that of individual trees. As a result, semivariance range values are consistently scaled to an appropriate window size.

#### Slope breaks

To overcome the need for user intervention in the determination of optimal window size, “slope breaks” were calculated. Slope breaks are a simple means of measuring a region of dependence around a pixel and are based on the assumption that every tree in an image may be a local maximum. For each pixel in the imagery, an omni-directional set of transects is analyzed from the central pixel to count the number of pixels until a minimum radiance value is reached. The slope break can also be described as the first inflection point in the gradient of reflectance around the tree. The mean value of the number of pixels to the slope reversal for all eight cardinal directions is used as a custom window size for that pixel (**Figure 2**). If the radiance of a pixel is lower than that of all surrounding pixels, a value of zero is assigned for the window size. The conversion from slope break value for a pixel to customized window size requires no user intervention.

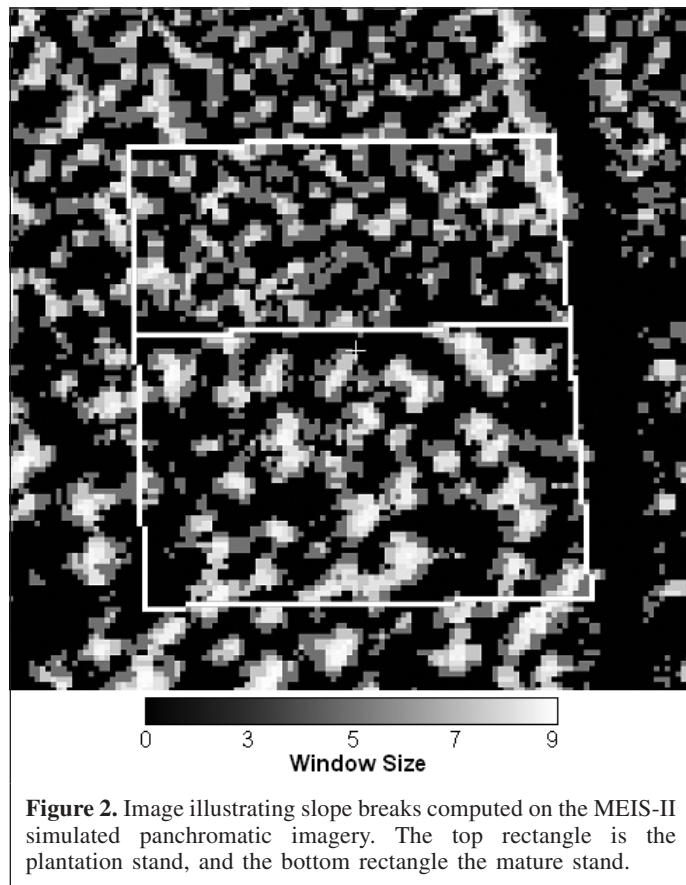


**Figure 2.** Image illustrating slope breaks computed on the MEIS-II simulated panchromatic imagery. The top rectangle is the plantation stand, and the bottom rectangle the mature stand.

### Spectral threshold and local variance within the LM window

One of the characteristics of the imagery is the occurrence of a random LM. To address selection of a random LM, we developed a filter that eliminates candidate LMs that fall below a user-specified minimum DN threshold and have a difference between minimum and maximum DN that is lower than a user-specified value. User investigation of a series of maximum grey level and minimum difference values is used to determine the most appropriate combination for a particular study location.

### Spatial dependence (Getis statistic)

In contrast to semivariance, the Getis statistic ( $G_i^*$ ) generates values that relate variations within patterns of spatial dependence. Thus, it has the potential to uncover discrete spatial-dependence characteristics that might be overlooked by existing techniques. Semivariance and  $G_i^*$  values are complementary techniques, with semivariance computing an indication of a region of pixel similarity and  $G_i^*$  results indicating the strength of pixel association within this region of spatial dependence.

Wulder and Boots (1998) have adapted the Getis statistic for processing remotely sensed imagery. Formulation and example calculation of  $G_i^*$  can be found in Wulder and Boots (1998; 2001). The Getis statistic,  $G_i^*$ , yields a standardized value that

indicates both the degree of autocorrelation in the DN values centred on a given pixel and the magnitude of these values in relation to those of the entire image. In consideration of remotely sensed imagery, the  $G_i^*$  values measure the extent to which a pixel is surrounded by a cluster of high or low values of the image DN values. Large positive  $G_i^*$  values denote a cluster of high DN values, and large negative  $G_i^*$  values a cluster of low DN values. In a high spatial resolution forestry context,  $G_i^*$  values indicate the spatial dependence within a tree crown or between shadow elements. High positive values generated from panchromatic image data indicate the presence of a tree object, whereas high negative values correspond to a non-tree feature (**Figure 3**). Accordingly,  $G_i^*$  values computed for near-infrared image data can be applied to assist in the screening for false positives generated from the radiance peak filtering routine. Further, as the  $G_i^*$  values are sensitive to the presence of tree objects, tree locations may be accentuated by the transformation of radiance values to  $G_i^*$  values. Processing the transformed  $G_i^*$  values for local maxima may allow for improved tree recognition. The ability to extract tree locations from radiance values transformed to  $G_i^*$  values is likely highly dependent on image spatial resolution, as the  $G_i^*$  values tend to form clusters from the radiance values (Wulder, 1999). As a result, processing  $G_i^*$ -transformed radiance values for LM may only be appropriate in high-resolution imagery where many pixels make up an individual tree crown.

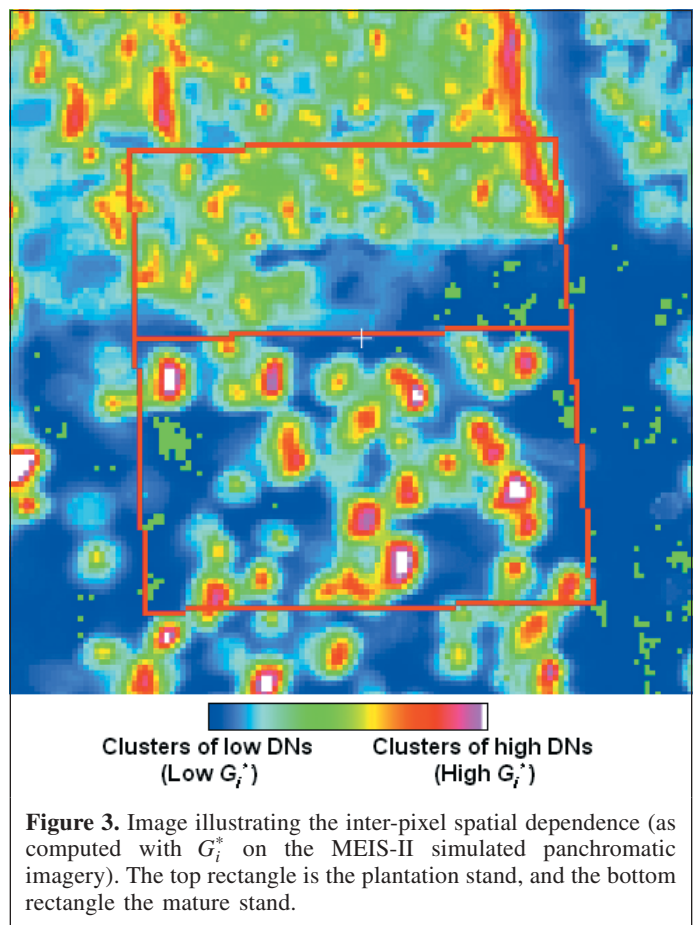


**Figure 3.** Image illustrating the inter-pixel spatial dependence (as computed with  $G_i^*$  on the MEIS-II simulated panchromatic imagery). The top rectangle is the plantation stand, and the bottom rectangle the mature stand.

### Spatial data threshold

The spatial-dependence threshold is based on an application of values of the Getis statistic as a threshold filter. Low  $G_i^*$  values indicate a cluster of low DN values, whereas high  $G_i^*$  values relate clusters of higher DNs. For each pixel that is identified as a potential LM, the  $G_i^*$  value at that location must be above zero for the LM to pass the threshold filter.

### LM filtering of spatial-dependence data

Passing the LM filter directly over the spatial-dependence data automatically applies the spatial-dependence threshold, as LMs are inherently greater than the defined threshold value. Additionally, the  $G_i^*$  will have a maxima value at the tree centre while also being surrounded by transformed values extending to the region of local dependence. The extent of the local spatial dependence indicated is variable and related to the size of the tree crowns present. High local  $G_i^*$  values will indicate centroids of local regions of spatial autocorrelation. The centroids indicated are representative of high panchromatic DN values over a region of local dependence.

## Results and discussion

### Fixed-sized LM filters with no error reduction applied

Prior to comparison of error reduction methods, a performance benchmark is required. In **Table 1** we present the proportion of correct, omitted (missed), and committed (falsely identified) trees for fixed-window LM filtering of image spectral data. (Omission is not noted in **Table 1** because omission level is simply the total number of trees minus the number of trees found.) The  $3 \times 3$  LM filter represents a superset of all possible LMs that can be isolated using a local maximum technique. The  $3 \times 3$  LM filter finds all local maxima, without regard to any image spatial structure and, as a result, the commission error is generally high. In an operational application, the detailed field data would likely not be present;

in that situation, there would be no way to detect false positives, resulting in an overestimation of stems. In this case the 67% accuracy overall must be taken in the context of 22% commission error; without the stem map developed for this study a 89% accuracy could be erroneously interpreted, as all trees “found” may be assumed to be correct. As a result, it is important to consider commission reduction in conjunction with the overall numbers of trees correctly identified.

The increase in window size from  $3 \times 3$  through  $5 \times 5$  to  $7 \times 7$  results in increasing omission errors for the plantation stand with less of an effect on the mature stand, indicating that data with resolution higher than 1 m are required for the detection of small trees. With a minimum of 33% of the plantation trees being missed with LM techniques in this study, it appears that 1-m imagery is too coarse for individual tree crown recognition in a Douglas-fir stand with crown radii less than 1.5 m. The mature stand, with an omission level of 20%, appears to have a stand structure that is more appropriate for LM filtering of 1-m spatial resolution imagery. The omission error may be interpreted as being largely a function of the image spatial resolution, whereas the commission error is related to the occurrence of spurious local maxima unrelated to elements of the crown canopy.

### Variable window sizes

Variable window sizes were applied to the LM filtering process in an attempt to reduce the level of commission error, or false positives, by integrating scene spatial structural information. Semivariance range and slope breaks are computed for each pixel and applied as a unique window size for that location. LM filtering with a variable window size determined by the semivariance method correctly located 64% of the trees in the entire stand and resulted in a commission error of 19% (**Table 1**). The lack of a consistent improvement in comparison to the fixed-window LM filtering is likely due to the selection of small window sizes from the same image spatial features that results in local maxima being found where

**Table 1.** Summary table of LM filtering results, including the benchmark in three static window sizes, and five spectral and spatial techniques.

Window size	Fixed window size			Variable-sized windows		Local variance test and threshold value	Variable window size with spatial-dependence ( $G_i^*$ ) threshold filter		Fixed window size processing of spatial-dependence ( $G_i^*$ ) data			Variable window size processing of spatial-dependence ( $G_i^*$ ) data	
	3	5	7	SVR	SB	3x3	SVR	SB	3	5	7	SVR	SB
All ( $n = 209$ )													
Correct	0.67	0.50	0.30	0.64	0.62	0.59	0.47	0.46	0.16	0.30	0.25	0.35	0.34
Commission	0.22	0.04	0.02	0.19	0.11	0.13	0.03	0.03	0.00	0.00	0.00	0.01	0.00
Plantation ( $n = 159$ )													
Correct	0.62	0.43	0.21	0.60	0.56	0.55	0.40	0.38	0.25	0.19	0.14	0.25	0.24
Commission	0.05	0.02	0.01	0.05	0.03	0.07	0.02	0.01	0.01	0.01	0.01	0.01	0.01
Mature ( $n = 50$ )													
Correct	0.80	0.72	0.60	0.76	0.80	0.70	0.70	0.74	0.66	0.64	0.60	0.66	0.66
Commission	0.78	0.10	0.08	0.64	0.38	0.32	0.08	0.10	0.00	0.00	0.00	0.00	0.00

**Note:**  $n$ , number of trees; SB, slope break dictated variable window size; SVR, semivariance range suggested variable window size.

no trees are present. Instead of a poorly fit window identifying spurious local maxima and resulting in a high commission level, variable-sized windows are being generated for the false positives. The LMs generated from slope breaks have fewer false positives than those from the semivariance range. The measurement of slope breaks from the imagery appears more sensitive to the actual extent of the crown. The semivariance range values, at the study image spatial resolution of 1 m, have a greater likelihood of generating stand-level information than individual crown information and thus are less locally adaptive.

The slope break suggested window-sized LM filter results illustrate a good relationship between number of trees correctly identified and commission level. For example, the commission for the mature stand is down from 78% with the fixed  $3 \times 3$  LM filter to 38% with the same number of trees correctly identified.

### Spectral threshold and local variance within the LM window

The application of a spectral threshold and local variance within the LM window resulted in an overall commission error level of 13% (**Table 1**). The low commission error of 7% for the plantation is expected, as the density of the stand, in conjunction with the spatial resolution, results in many LM hits. More importantly, for the mature stand, where the opportunity for commission is greater because of the tree size and large spaces between the trees, a false positive rate of 32% is found. The 32% level of false positives for the LM filter with a threshold and local variance test is an improvement over the use of a fixed  $3 \times 3$  window with no additional screening, yet the level correct is less than that found for the fixed-window analysis. For the mature stand, using the spectral threshold with the local variance test, the commission level is better than that for the variable window size dictated from slope breaks. Yet the level correct for the mature stand with the spectral threshold and local variance method (at 70%) is lower than that with the 80% correct computed for the variable window sizes from slope breaks.

### Spatial-dependence threshold

The spatial-dependence filtering results in a reduction in commission error in relation to the unfiltered results (**Table 1**). A good relationship between number of trees correctly identified is evident for the mature stand, where correct levels are high and commission is low. Yet, the overall correct level is low, too low to make up for the low commission level.

The stratification of the results based on the tree age and size distribution demonstrates superior results for the larger mature trees compared with those for the smaller plantation trees. Up to 74% of the larger mature trees are accounted for, whereas the maximum success rate is 40% for the smaller plantation trees. The desired use of the resultant tree locations from the LM filtering will dictate what are acceptable levels of success. For example, this high omission rate may be acceptable if the use of the tree locations is for subsequent signature extraction or basal area estimation. The success of the LM filter based on  $G_i^*$

values to decrease the commission error indicates a potential for directly processing the  $G_i^*$  values for local maxima.

### LM filtering of spatial-dependence data

The application of  $G_i^*$  values as a threshold filter in conjunction with an LM filter indicated the potential for direct processing of the spatial-dependence values with an LM filter to isolate individual trees to aid in the reduction of commission error. The result of processing the spatial-dependence values with fixed-sized LM filters is presented in **Table 1**. The success rates vary by window size and stand age. The tendency of  $G_i^*$  values to represent clusters of similar DN values (Wulder and Boots, 1998; Wulder, 1999) results in a loss of individual tree location detail, especially in the dense plantation stand. The clustering effect is clearly demonstrated for a  $3 \times 3$  LM filter on the panchromatic data, illustrated with the results over all age classes with a success level of 16%. An increase in window size results in an improvement in the number of trees correctly identified, which relates to the size of the domain of the spatial process. The variable-sized windows when applied to the spatial-dependence data result in more consistent levels of success (**Table 1**), with successful identification of trees occurring at a rate of approximately 35%. Successful identification of trees increases as the sizes of the trees increase. The relatively low rate of tree identification is aided by the low amount of commission error. Locations that are identified with the LM filtering of the spatial-dependence values are almost invariably trees.

The low, to absent, commission error is related to the manner in which the radiance values are transformed into  $G_i^*$  values, with the clusters of high DN values becoming high  $G_i^*$  values. The high  $G_i^*$  values, accordingly, when processed with an LM filter, act similarly to the  $G_i^*$  thresholded results. As with the results for the LM filter suite processed with a  $G_i^*$  threshold filter, the desired use of the digitally isolated trees will dictate the success of the LM isolation. The low commission error is of concern if the identified trees are to be utilized for further analysis. For example, the LM-located trees may be appropriate for signature development for multispectral classification of the trees. Further, at the 1-m spatial resolution the large trees are being found with the LM filtering method. An analysis of the distribution of the error by the size of the tree is presented in Wulder et al. (2000).

## Conclusions

The efficacy of a given error reduction method must be considered in the context of the number of trees that are correctly identified. When considering the number of trees correctly identified, the size of the trees found must be considered in relation to the image spatial resolution. Small trees, below the range of detection given the spatial resolution available, are beyond the scope of these error reduction methods. Yet, for large trees, which are more readily detectable, omission and commission are more significant. Our creation of

a detailed stem map allowed for the reporting of omission and commission error; without a detailed stem map, the committed trees may be incorrectly assumed to be legitimate.

The comparison of error reduction methods must be kept in reference to the comments made earlier. The success, or failure, of a given method is not indicated from commission level alone; the proportion correct must also be considered. The goal of the particular LM analysis, that is, what are the stems required for, must also be kept in mind. The error rates found for the plantation stand are largely a function of the image spatial resolution, and little can be done to recover sub-pixel trees. The limits to the plantation results are also an issue when interpreting the results over both stands combined. When considering the entire stand, favorable results are found for the variable window size techniques and the threshold-within-window variance filters. For the mature stand, with large crown sizes, application-appropriate results are found for the spatial-dependence filtering of LM generated within windows of sizes suggested by local slope breaks, where the correct proportion is high (74%) and the false positive level is low (10%). The results related to the mature stand indicate that when many pixels make up an individual crown, LM detection is possible, as are several means for reducing the number of falsely indicated trees.

## Acknowledgements

The authors wish to thank Geoff Hay, who rigorously collected the field data utilized in this study, and Gordon Joyce of the Greater Victoria Watershed District Office for allowing us to conduct research in the watershed. Three anonymous reviewers are also thanked for many insightful comments and excellent suggestions that improved this manuscript.

## References

- Culvenor, D. 2002. TIDA: An algorithm for the delineation of tree crowns in high spatial resolution remotely sensed imagery. *Computers & Geosciences*, Vol. 28, No. 1, pp. 33–44.
- Curran, P., and Atkinson, P. 1998. Geostatistics and remote sensing. *Progress in Physical Geography*, Vol. 22, No. 1, pp. 61–78.
- Dralle, K., and Rudemo, M. 1997. Stem number estimation by kernel smoothing of aerial photos. *Canadian Journal of Forest Research*, Vol. 26, pp. 1228–1236.
- Franklin, S., Wulder, M., and Lavigne, M. 1996. Automated derivation of geographic windows for use in remote sensing digital image analysis. *Computers & Geosciences*, Vol. 22, No. 6, pp. 665–673.
- Gougeon, F. 1995a. Comparison of possible multispectral classification schemes for tree crowns individually delineated on high spatial resolution MEIS images. *Canadian Journal of Remote Sensing*, Vol. 21, No. 1, pp. 1–9.
- Gougeon, F. 1995b. A crown-following approach to the automatic delineation of individual tree crowns in high spatial resolution digital images. *Canadian Journal of Remote Sensing*, Vol. 21, No. 3, pp. 274–284.
- Hay, G., and Niemann, K. 1994. Visualizing 3-D texture: a three-dimensional approach to model forest texture. *Canadian Journal of Remote Sensing*, Vol. 20, No. 2, pp. 89–101.
- Hugh Hamilton, Ltd. 1991. *Greater Victoria water district watershed management forest cover classification, Sooke Lake Watershed, scale 1 : 10 000*. Hugh Hamilton, Ltd., Vancouver, B.C.
- Hyypä, J., Hyypä, H., Inkinen, M., Engdahl, M., Linko, S., and Zhu, Y. 2000. Accuracy comparison of various remote sensing data sources in the retrieval of forest stand attributes. *Forest Ecology and Management*, Vol. 128, Nos. 1–2, pp. 109–120.
- Larsen, M. 1999. Finding an optimal match window for spruce top detection based on an optical tree model. In *Proceedings of the International Workshop on Automated Interpretation of High Spatial Resolution Digital Imagery for Forestry*, 10–12 Feb. 1998, Victoria, B.C. Edited by D. Hill and D. Leckie. Natural Resources Canada, Canadian Forest Service, Pacific Forestry Centre, Victoria, B.C. pp. 55–66.
- Larsen, M., and Rudemo, M. 1997. Using ray-traced templates to find individual trees in aerial photos. In *Proceedings of the 10th Scandinavian Conference on Image Analysis*, 9–11 June 1997, Lappeenranta, Finland. pp. 1007–1014.
- Leckie, D., Yaun, X., Ostaff, D., Piene, H., and MacLean, D. 1992. Analysis of high spatial resolution multispectral MEIS imagery for Spruce Budworm damage assessment on a single tree basis. *Remote Sensing of Environment*, Vol. 40, No. 2, pp. 125–136.
- Li, X., and Strahler, A. 1992. Geometric-optical bidirectional reflectance modeling of the discrete crown vegetation canopy: effect of crown shape on mutual shadowing. *IEEE Transactions on Geoscience and Remote Sensing*, Vol. 30, No. 2, pp. 276–291.
- Mangold, R. 1999. IKONOS has arrived. *EOM*, Vol. 8, No. 9, p. 7.
- Pinz, A. 1999. Tree isolation and species classification. In *Proceedings of the International Workshop on Automated Interpretation of High Spatial Resolution Digital Imagery for Forestry*, 10–12 Feb. 1998, Victoria, B.C. Edited by D. Hill and D. Leckie. Natural Resources Canada, Canadian Forest Service, Pacific Forestry Centre, Victoria, B.C. pp. 127–140.
- Pollock, R. 1996. *The automatic recognition of individual trees in aerial images of forests based on a synthetic tree crown image model*. Ph.D. thesis, Department of Computer Science, University of British Columbia, Vancouver.
- Tahu, G., Baker, J., and O'Connell, K. 1998. Expanding global access to civilian and commercial remote sensing data: implications and policy issues. *Space Policy*, Vol. 14, pp. 179–188.
- Till, S., McColl, W., and Neville, R. 1983. Development, field performance and evaluation of the MEIS-II multi-detector electro-optical scanner. In *Proceedings of the 17th International Symposium on Remote Sensing of Environment*, 9–13 May 1983, Ann Arbor, Mich. pp. 1137–1146.
- Walsworth, N., and King, D. 1999. Comparison of two tree apex delineation techniques. In *Proceedings of the International Workshop on Automated Interpretation of High Spatial Resolution Digital Imagery for Forestry*, 10–12 Feb. 1998, Victoria, B.C. Edited by D. Hill and D. Leckie. Natural Resources Canada, Canadian Forest Service, Pacific Forestry Centre, Victoria, B.C. pp. 93–104.
- Wulder, M. 1999. Image spectral and spatial information in the assessment of forest structural and biophysical data. In *Proceedings of the International Forum on Automated Interpretation of High Spatial Resolution Digital Imagery for Forestry*, 10–12 Feb. 1998, Victoria, B.C. Pacific Forestry Centre, Canadian Forest Service, Natural Resources Canada, Victoria, B.C. pp. 267–281.

- Wulder, M., and Boots, B. 1998. Local spatial autocorrelation characteristics of remotely sensed imagery assessed with the Getis statistic. *International Journal of Remote Sensing*, Vol. 19, No. 11, pp. 2223–2231.
- Wulder, M., and Boots, B. 2001. Local spatial autocorrelation characteristics of Landsat TM imagery of managed forest area. *Canadian Journal of Remote Sensing*, Vol. 27, No. 1, pp. 67–75.
- Wulder, M., LeDrew, E., Lavigne, M., and Franklin, S. 1998. Aerial image texture information in the estimation of northern deciduous and mixed wood forest leaf area index (LAI). *Remote Sensing of Environment*, Vol. 64, pp. 64–76.
- Wulder, M., Niemann, O., and Goodenough, D. 2000. Local maximum filtering for the extraction of tree locations and basal area from high spatial resolution imagery. *Remote Sensing of Environment*, Vol. 73, pp. 103–114.